Dopant and Defect Issues in Oxide and Nitride Semiconductors

Cambridge University Press
978-1-107-40869-2 - Semiconductor Defect Engineering–Materials, Synthetic Structures and Devices II: Symposium held April 9-13, 2007, San Francisco, California, U.S.A.
Edited by S. Ashok, J. Chevallier, P. Kiesel and T. Ogino
Excerpt
More information

Mater. Res. Soc. Symp. Proc. Vol. 994 © 2007 Materials Research Society 0994-F01-03

Arsenic in ZnO and GaN: Substitutional Cation or Anion Sites?

Ulrich Wahl[1,2], Joao Guilherme Correia[1,2], Elisabete Rita[2], Ana Claudia Marques[2,3], Eduardo Alves[1,2], Jose Carvalho Soares[2], and The ISOLDE Collaboration[3]
[1]Dep. Fisica, Instituto Tecnologico e Nuclear, Estrada Nacional 10, Sacavem, 2686-953, Portugal
[2]Centro de Fisica Nuclear da Universidade de Lisboa, Av. Prof. Gama Pinto 2, Lisbon, 1649-003, Portugal
[3]CERN, Geneva 23, 1211, Switzerland

ABSTRACT

We have determined the lattice location of ion implanted As in ZnO and GaN by means of conversion electron emission channeling from radioactive ^{73}As. In contrast to what one might expect from its nature as a group V element, we find that As does *not* occupy substitutional O sites in ZnO but in its large majority substitutional Zn sites. Arsenic in ZnO is thus an interesting example for an impurity in a semiconductor where the *major* impurity lattice site is determined by atomic size and electronegativity rather than its position in the periodic system. In contrast, in GaN the preference of As for substitutional cation sites is less pronounced and about half of the implanted As atoms occupy Ga and the other half N sites. Apparently, the smaller size-mismatch between As and N and the chemical similarity of both elements make it feasible that As partly substitutes for N atoms.

INTRODUCTION

Modifying the properties of ZnO and GaN by means of incorporating group V impurities is of interest in both of these wide band gap semiconductors, although for different reasons. In the case of the technologically promising II-VI compound ZnO, besides N [1,2] the heavy group-V elements P [1,2], As [2-9], and Sb [10-12] have been reported in the literature as possible *p*-type dopants. However, there is an ongoing debate whether for P, As, and Sb the *p*-type character results from these impuritities simply replacing O atoms, thus acting as simple "chemical" dopants [3,4,8], or is due to the formation of more complicated defect complexes [9,12-14]. The relative sizes of Zn, O and P, As, or Sb atoms favour incorporation of the heavy group-V elements on cation sites. Theoretical calculations have suggested that the acceptor action of arsenic in ZnO results from its incorporation on Zn sites in the form of electrically active $As_{Zn}–2V_{Zn}$ complexes [13-14]. If this hypothesis were correct, the intentional introduction of such a particular defect would constitute a novel approach to semiconductor doping and present a challenging task for defect engineering.

In the case of GaN, the doping with As has been studied with respect to its luminescence behaviour [15-22] and, at higher concentrations, with regards to the formation of $GaAs_xN_{1-x}$ alloys and the related modification of the GaN band gap [17,21,23-26].

Unfortunately the growth of $GaAs_xN_{1-x}$ compounds encounters significant difficulties, one of the reasons being that the most stable polytype of GaN is hexagonal wurtzite while GaAs crystallizes in the cubic zinc blende structure. However, while, on the As-rich side of the phase diagram, it is possible to incorporate up to ~10-15% of N into cubic GaAs [27,28], on the N-rich side not more than ~1% of As in GaN have been achieved [23-26]. In the intermediate region usually the coexistence of hexagonal N-rich GaAsN and cubic As-rich GaNAs phases is observed. As a matter of fact, arsenic in GaN has been suggested to act as an amphoteric impurity, with its lattice site preference depending on the doping character of the material, i.e. mostly substitutional Ga in *p*-type but also substitutional N in *n*-type [29,30].

In order to understand the properties of the heavy group V impurities in ZnO and GaN it is hence essential to assess whether they prefer substitutional cation or anion sites. However, so far only few experimental methods have been able to provide reliable knowledge on the lattice sites of these elements in ZnO and GaN. Desnica et al [31,32] concluded from Mössbauer effect studies that ^{119}Sb implanted into GaN is incorporated in substitutional Ga sites. Since their finding was in contrast to all common III-V compounds, where Sb group V foreign atoms occupy the anion site, they termed Sb_{Ga} an "antisite" defect, in analogy to As_{Ga} antisites, a native defect commonly observed at low concentrations in GaAs crystals. We summarize here recent results on lattice location experiments of radioactive ^{73}As in ZnO [33,34] and GaN [35] by means of the emission channeling technique [36], giving direct evidence that As prefers Zn sites in ZnO and acts as an amphoteric impurity in GaN.

EXPERIMENT

A typical emission channeling experiment is schematically illustrated in figure 1. The method uses radioactive probe atoms that have been implanted into a single crystal sample and is based on the fact that charged particles from the nuclear decay (in our case conversion electrons) experience channeling or blocking effects along major crystallographic axes and planes. The resulting anisotropic emission yield from the crystal surface characterizes the lattice site occupied by the probe atoms during decay.

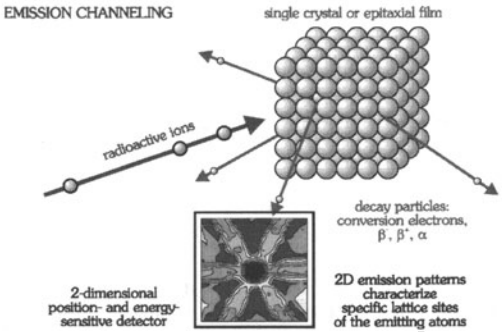

Figure 1. Illustration of a typical emission channeling experiment using radioactive probe atoms implanted into a sample. Note that the size of the single crystal is of course greatly exaggerated in comparison to the detector. Also, many atomic layers contribute to the channeling effect.

For the experiments described below, single crystalline thin films (thickness ~1 µm) of GaN grown on sapphire and a [0001] oriented ZnO single crystal were implanted at room temperature with ^{73}As ($t_{1/2}$= 80.3 d) at 60 keV energy with fluences between 0.8-7.0×10^{13} cm^{-2}. The production of ^{73}As and the implantation were performed at CERN's on-line isotope separator facility ISOLDE. The As depth profile corresponding to these implantation conditions is centered at a depth of 232 Å, with a straggling of 100 Å and the As peak concentration amounts to 0.3-2.7×10^{18} atoms cm^{-3}. The maximum As concentration in our experiments was hence still in the 30 ppm regime. The angular emission patterns of the 42.3 keV and 52.1 keV conversion electrons from the ^{73}As → ^{73}Ge decay were recorded around the [0001], $[\underline{1}102]$, $[\underline{1}101]$ and $[\underline{2}113]$ directions by means of a 3×3 cm^2 sized 22×22 pixel position-sensitive Si detector [37,38] at a distance of 30 cm from the sample. These measurements were carried out at room temperature in the as-implanted state and following 10 min *in situ* vacuum (<10^{-5} mbar) annealing steps at 300°C, 600°C and 900°C.

The evaluation of the probe atom lattice location was performed by quantitatively comparing the experimental patterns with theoretical ones for different lattice sites, using the two-dimensional fit procedure outlined in Ref. [37]. In the fit procedure, we considered theoretical patterns resulting from emitter atoms at substitutional cation (i.e. S_{Zn} and S_{Ga}) and anion sites (i.e. S_O and S_N) with varying root mean square (rms) displacements, the main interstitial sites (figure 2, see also Refs. [33,39]), and a diversity of interstitial sites resulting from displacements along or off the *c*-axis. The theoretical emission channeling patterns were calculated by means of the "manybeam" theory of electron diffraction in single-crystals [36]. Details with respect to the structural properties of GaN and ZnO used in the simulations have been given previously [39-41].

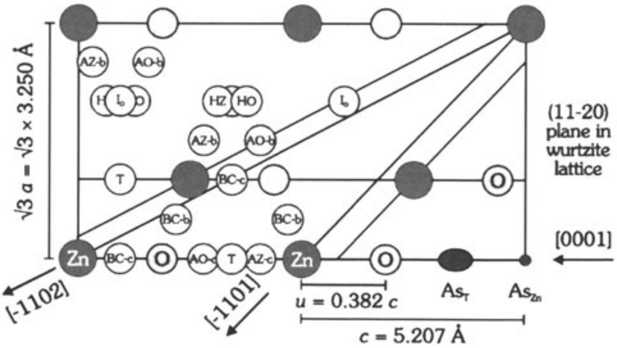

Figure 2. The $(11\underline{2}0)$ plane in the ZnO wurtzite lattice, showing the location of substitutional Zn sites, substitutional O sites, bond center BC, antibonding Zn (AZ) and antibonding O (AO), interstitial "octahedral" (I_O), "tetrahedral" (T) and "hexagonal" (HZ and HO). "-c" denotes sites within and "-b" basal to the *c*-axis. The small red circle and larger ellipse in the lower right hand corner indicate the estimated experimental error in determining the location of ^{73}As atoms on substitutional Zn and interstitial T sites from the emission channeling experiments.
From Ref. [33]. © The American Physical Society 2005.

RESULTS

Lattice location of As in ZnO

Figure 3 shows typical angular distribution patterns of conversion electrons in the vicinity of the four major crystalline directions of the ZnO sample. The patterns were measured at room temperature after 600°C annealing but are in fact very similar to what is observed already in the as-implanted state (shown in Ref. [34]) or after 300°C annealing (shown in Ref. [33]). The best fit of theoretical patterns to the experimental ones was obtained for 80(7)% of probe atoms at S_{Zn} sites, and the remainder on "random" sites (random sites are lattice positions which cause only negligible anisotropy in the emission patterns, for instance probe atoms in positions of very low symmetry or in heavily damaged surroundings). The rms displacements from the ideal Zn positions were in all cases around 0.07–0.17 Å, i.e. somewhat larger than the thermal vibration amplitude of the Zn atoms, u_1(Zn)=0.080 Å. Major fractions of emitter atoms on other high-symmetric lattice sites can be ruled out. The theoretical channeling patterns from emitter atoms on substitutional O sites, for instance, are similar to those resulting from substititutional N sites in GaN shown below in figure 4 (m-n) and are clearly incompatible with the experimental patterns. Including additional fractions of emitter atoms on S_O sites (besides S_{Zn} and random sites) in the fits, the resulting fractions were smaller than 5% percent, which is within the error bars of the accuracy of the method.

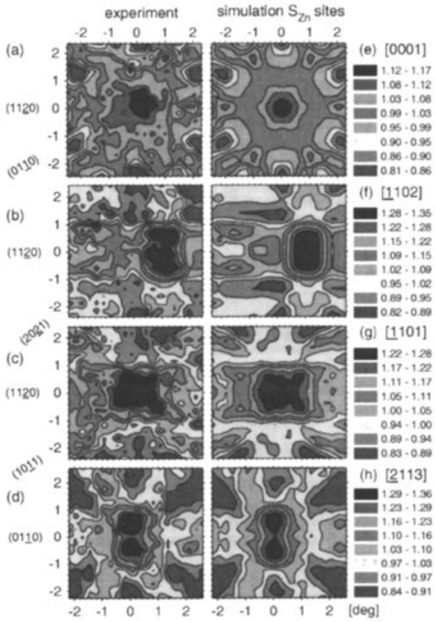

Figure 3. Angular distribution of conversion electrons from ^{73}As in ZnO following 600°C annealing around the [0001] (a), [$\underline{1}$102] (b), [$\underline{1}$101] (c) and [$\underline{2}$113] (d) axis. (e-h): best fits of the channeling patterns for each direction, corresponding to 80(7)% of probe atoms at S_{Zn} sites.

In contrast to all experimental channeling patterns in the as-implanted state and following 300°C and 600°C vacuum annealing, which could be very well fitted assuming only As on substitutional Zn sites and on random sites, following 900°C vacuum annealing an additional lattice site had to be introduced in the fits. Whereas the [0001] patterns remained relatively unaltered, showing that the probe atoms were still well-aligned with the c-axis, satisfactory fit results for the off-surface directions [$\underline{1}$102], [$\underline{1}$101] and [$\underline{2}$113] could only be obtained when also ^{73}As atoms located within 0.4 Å from tetrahedral interstitial T sites were allowed in the fits [33]. Note that the T sites are the major interstitial sites in the wurtzite structure that are aligned with the c-axis, making their [0001] emission channeling pattern identical to those of S_{Zn} and S_O sites.

Lattice location of As in GaN

Following implantation of ^{73}As in GaN, the experimental channeling patterns could not be satisfactorily described by As on cation sites only.

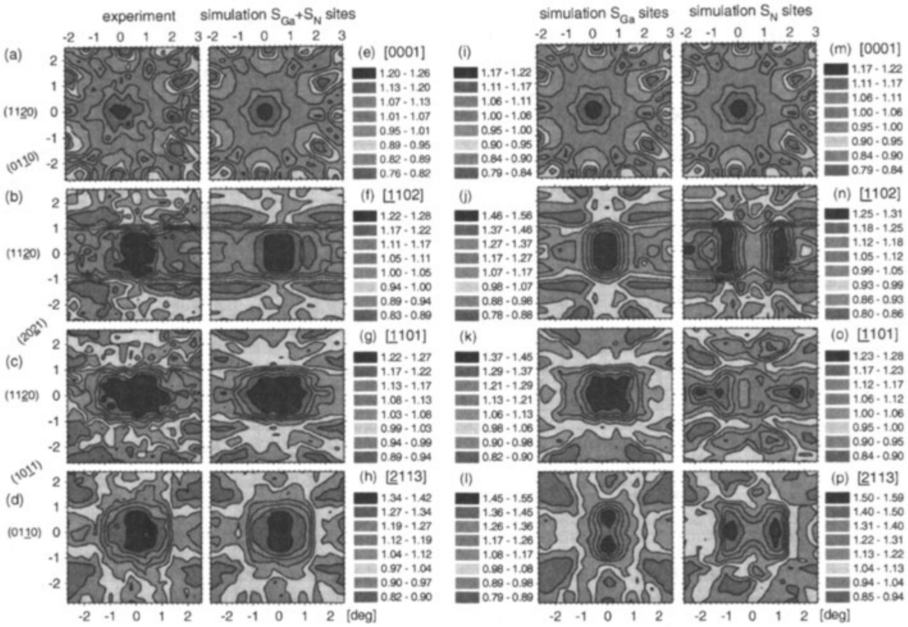

Figure 4. Experimental emission channeling patterns from ^{73}As in GaN in the as-implanted state around the [0001] (a), [$\underline{1}$102] (b), [$\underline{1}$101] (c) and [$\underline{2}$113] (d) axis. (e-h): best fits of the channeling patterns for each direction, corresponding to 62(5)% of probe atoms at S_{Ga} and 45(3)% at S_N sites. Panels (i-l) are theoretical patterns for 100% of emitter atoms on S_{Ga} sites and panels (m-p) for 100% on S_N sites. Note that the [0001] patterns for S_{Ga} and S_N are identical since both sites are aligned with the atomic rows along the c-axis.

As an example we have given in figure 4 (a-d) above the emission channeling patterns measured in the as-implanted state, which are compared to theoretical patterns for 100% of emitter atoms on substitutional Ga sites [figure 4 (i-l)] and for 100% on substitutional N sites [figure 4 (m-p)]. The comparison of experimental and theoretical patterns shows that the measured emission channeling effects are certainly dominated by emitter atoms on Ga sites, which either produce relatively strong and wide axial effects or a close double peak in case of the [$\underline{2}113$] axis. In contrast, emitter atoms on N sites are characterized by multiple-peak effects which are generally quite far apart and weaker. Obviously, there are certain features in the experimental patterns which cannot be explained by As on Ga sites alone but require the presence of substantial amounts of As on N sites. Most obvious in that respect are the [$\underline{2}113$] patterns, where pure Ga sites would result in an intense close double peak within the ($1\underline{2}12$) plane [vertical in figure 4 (l)], while N sites would be characterized by a pronounced double peak within the ($01\underline{1}0$) plane [horizontal in figure 4 (p)]. What is actually observed in the experiment is a superposition of the Ga and N site patterns, with the best fits obtained for 62(5)% of As on Ga sites and 45(3)% on N sites. In comparsion to the fit results assuming pure Ga site occupation, the chi square of the [$\underline{1}102$], [$\underline{1}101$] and fits improved by 39%, 29% and 65% upon introducing the fraction of emitter atoms on substitutional N sites. The rms displacements of As from the ideal S_{Ga} and S_N sites could not be independently derived in an unambiguous way from the fit results, however, both were in the range ~0.08-0.19 Å, somewhat larger than the thermal vibration amplitudes of Ga (0.074 Å) and N (0.081 Å) and corresponding to 4–10% of the bond length of $b = 1.937$ Å in GaN.

Comparison of ZnO and GaN as a function of annealing temperature

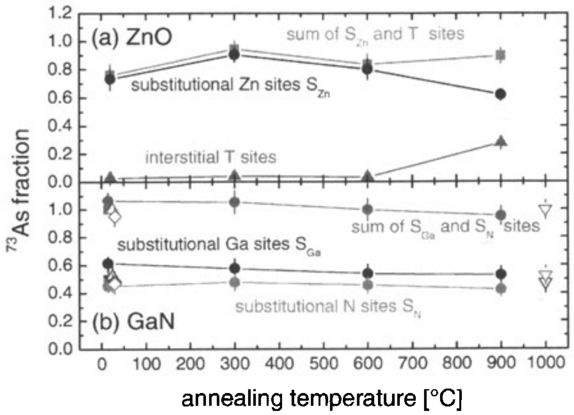

Figure 5. Fitted fractions of ^{73}As probe atoms on the considered lattice sites in ZnO (a) and GaN (b) as a function of annealing temperature. The four different symbols (circles, squares, triangles and diamonds) in panel (b) correspond to four different GaN crystals investigated, of which only one was subjected to a full annealing sequence, while the other three were only studied in the as-implanted state or following 1000°C treatment. All annealings were for 10 min under vacuum except for the GaN sample annealed at 1000°C, which was under N_2 atmosphere for 30 min.

Figure 5 above summarizes and compares the lattice location results for ^{73}As in ZnO and GaN as a function of annealing temperature. In both cases quite high fractions of probe atoms occupied regular, high-symmetric (i.e. non-random) lattice sites already in the as-implanted state. Correspondingly, major annealing steps, which would be characterized by a further increase in these fractions, were absent. Apart from the partial site change from S_{Zn} to interstitial T sites, which occurred during 900°C annealing in ZnO, the fractions were quite stable. In one GaN sample the sum of all fitted fractions is somewhat higher than 100%. This is due to an experimental uncertainty which is introduced when correcting for the background of scattered electrons (±1/10 of each fraction), and affects all fractions in the same way. The fraction of As on N sites appears to be somewhat higher in the GaN sample which was subjected to 1000°C annealing, which might indicate that high-temperature treatment can influence to some extent the preferred lattice site of As. However, the difference is relatively small and more experiments would be needed in order to confirm whether this is a significant effect.

DISCUSSION

Based on the results of their Mössbauer effect studies, which suggested the incorporation of implanted Sb on Ga sites in GaN, Desnica et al proposed that, besides chemical similarities, the atomic or ionic size of an impurity can play a decisive role in determining its preferred lattice site [31,32]. Similar arguments were put forward by Pearton et al [1] regarding the incorporation of the heavy group V elements P, As and Sb in ZnO. It was argued that the large ionic size of these impurities in their 3– charge state would prohibit their incorporation on substitutional O sites, while the much smaller ionic size of the 3+ charge state would favor replacing the Zn^{2+} ions. In table I we compare the various relevant ionic and covalent radii of the elements under consideration, giving in addition their Pauling electronegativity, which can be used as a rough criterion for chemical similarity. As is obvious from these data, the substitution of an O^{2-} (1.38 Å) ion by As^{3-} (2.22 Å) would heavily disturb the ZnO lattice. On the other hand, the much smaller size of As^{3+} (0.58 Å) provides an almost perfect replacement for Zn^{2+} ions (0.60 Å). This is schematically illustrated in figure 6. In addition, the difference in the electronegativity of As and Zn (0.4) is smaller than the difference between As and O (1.5), so that in this case our experimental findings regarding the preference of As for Zn sites can be well explained on the basis of such relatively simple considerations. The preference of As and Sb for Zn sites has also been proposed by Limpijungnong et al [13,14] based on results of first-principles calculations using the local density approximation. These authors suggested in addition that the experimentally observed p-type character of As- or Sb-doped ZnO results from the formation of As_{Zn}–$2V_{Zn}$ or Sb_{Zn}–$2V_{Zn}$ complexes, which act as structural acceptors, in contrast to the simple "chemical" acceptors As_O or Sb_O. The implications of our experimental observations with respect to distinguishing between these two models is discussed in a separate section below.

Table I. Pauling electronegativity, covalent radius, relevant charge states and corresponding ionic radii for the host elements Zn, Ga, N, O and the group V impurities P, As and Sb. The ionic radii are from: [1] Ref. [42] for coordination number IV, [2] Ref. [42] for coordination number VI, [3] Ref. [43] for coordination number VI

Element	Pauling electro-negativity	covalent radius [Å]	charge state	ionic radius [Å]
Zn	1.6	1.25	2+	0.60[1]
O	3.5	0.73	2-	1.38[1]
Ga	1.6	1.26	3+	0.47[1]
N	3.0	0.75	3-	1.46[1]
P	2.1	1.06	3- 3+ 5+	2.12[3] 0.44[2] 0.17[1]
As	2.0	1.20	3- 3+ 5+	2.22[3] 0.58[2] 0.335[1]
Sb	1.9	1.40	3- 3+ 5+	2.45[3] 0.74[1] 0.60[2]

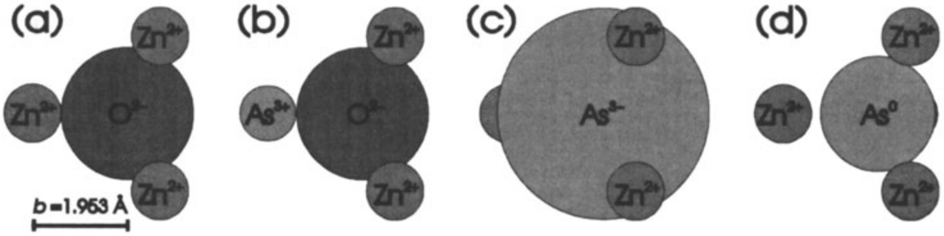

Figure 6. Schematics illustrating the ionic sizes of Zn, O and As in zinc oxide. Note that the structure has been rotated in such a way that the straight line connecting the central O or As atom with the leftmost atom lies within the horizontal plane. (a): In the undisturbed ZnO lattice, the bond length b = 1.953 Å between neighboring Zn and O atoms almost exactly matches the sum of the ionic radii of Zn^{2+} (0.60 Å) and O^{2-} (1.38 Å), illustrating the comparatively strong ionic character of the bonds. (b): The leftmost Zn^{2+} ion has been replaced with an As^{3+} ion of radius of 0.58 Å, illustrating the good size match between As^{3+} and Zn^{2+}. (c): An As^{3-} ion with its large radius of 2.22 Å does not fit within the cage of the surrounding four Zn^{2+} ions. (d): In contrast, a neutral As^0 atom with its covalent radius of 1.20 Å would fit within the cage of the surrounding four Zn^{2+} ions.

The case of As in GaN is somewhat different. In GaN, the ionic radii of As^{3+} and Ga^{3+} are also well matched (0.58 Å vs 0.62 Å), while the size-mismatch between the As^{3-} and N^{3-} anions is considerably smaller (2.22 Å vs 1.71 Å) than in ZnO but still significant. The electronegativity